NANO LETTERS

2006
Vol. 6, No. 10
2177−2183

Biotemplated Nanopatterning of Planar Surfaces with Molecular Motors

Cordula Reuther,[†] Lukasz Hajdo,[‡] Robert Tucker,[§] Andrzej A. Kasprzak,[‡] and Stefan Diez*,[†]

Max-Planck-Institute of Molecular Cell Biology and Genetics, Pfotenhauerstrasse 108, 01307 Dresden, Germany, The Nencki Institute of Experimental Biology, Pasteur 3, 02-093 Warsaw, Poland, and University of Florida, Gainsville, Department of Materials Science and Engineering, 160 Rhines Hall, Gainesville, Florida 32611-6400

Received April 25, 2006; Revised Manuscript Received July 27, 2006

ABSTRACT

We report on the generation of nanometer-wide, non-topographical patterns of proteins on planar surfaces. In particular, we used the regular lattice of reconstituted microtubules as template structures to specifically bind and transfer kinesin-1 and nonclaret disjunctional motor proteins. The generated tracks, which comprise dense and structurally oriented arrays of functional motor proteins, proved to be highly efficient for the guiding of microtubule transporters.

Biomolecular motors are currently explored for an increasing number of applications in hybrid bionanodevices.[1] Along these lines, gliding motility assays, where reconstituted microtubule filaments are propelled over a substrate by surface-attached motor proteins, have been used to transport micrometer- and nanometer-sized objects, such as small beads,[2] quantum dots[3] or DNA molecules.[4] However, one prerequisite for controllable nanotransport is the reliable guiding of filament movement along predefined paths, a challenging task that has recently been achieved only via costly and labor-intensive topographical surface modifications.[2,5−10] Here, we report on the generation of nanometer-wide, non-topographical tracks of motor proteins. In particular, we used the regular lattice of reconstituted microtubules as template structures to specifically bind and transfer kinesin-1 and nonclaret disjunctional (Ncd) motor proteins on planar surfaces. Through this approach, which has been inspired by biological transport systems found within cells, dense and structurally oriented arrays of functional motor proteins were created. The motor tracks proved to be highly efficient for the guiding of microtubule transporters.

Microtubules are cytoskeletal filaments 25 nm in diameter and several micrometers long. Their lattice displays an 8 nm periodicity originating from the size of the dimeric tubulin proteins that make up the protofilaments. We investigated two different methods of biotemplated nanopatterning of planar surfaces with motor proteins: "biotemplated stamping" (Figure 1a) and "biotemplated binding" (Figure 1b). In the stamping approach, kinesin-1 molecules were bound in solution with their motor domains to "template" microtubules in the absence of ATP. The generated complexes were then adsorbed onto the surface (step I), and ATP was added in order to propel the template microtubules off the surface-bound motor proteins. This way, tracks of oriented motor molecules, with their motor domains pointing away from the surface, were generated (step II). In the binding approach, the template microtubules were first immobilized on the surface (step I). Kinesin-1 or Ncd motor proteins were then specifically bound to the template microtubules via specific linker molecules or the second microtubule binding site in their tail domain, respectively (step II). For both approaches, based on either biotemplated stamping or binding, the addition of "transport" microtubules in a motility solution containing ATP led to guided movement along the motor tracks (step III).

Experiments on the microtubule-assisted stamping and binding of motor proteins were performed in 2-mm-wide flow cells self-built from two coverslips (Corning, 22 × 22 mm^2 and 18 × 18 mm^2) and two pieces of double-sided sticking tape (Scotch 3M, thickness 0.1 mm). Microtubules were polymerized from 5 μL of bovine brain tubulin (4 mg/mL; labeled with different fluorophores as stated below) in BRB80 buffer (80 mM potassium PIPES, pH 6.9, 1 mM EGTA, 1 mM $MgCl_2$) with 4 mM $MgCl_2$, 1 mM Mg-GTP, and 5% DMSO at 37 °C. After 30 min, the microtubule polymers were stabilized and diluted 100-fold in room-temperature BRB80 containing 10 μM taxol. Fluorescent images were obtained using a Zeiss Axiovert 200M inverted

* Corresponding author. E-mail: diez@mpi-cbg.de.
[†] Max-Planck-Institute of Molecular Cell Biology and Genetics.
[‡] The Nencki Institute of Experimental Biology.
[§] University of Florida.

10.1021/nl060922l CCC: $33.50
Published on Web 09/01/2006

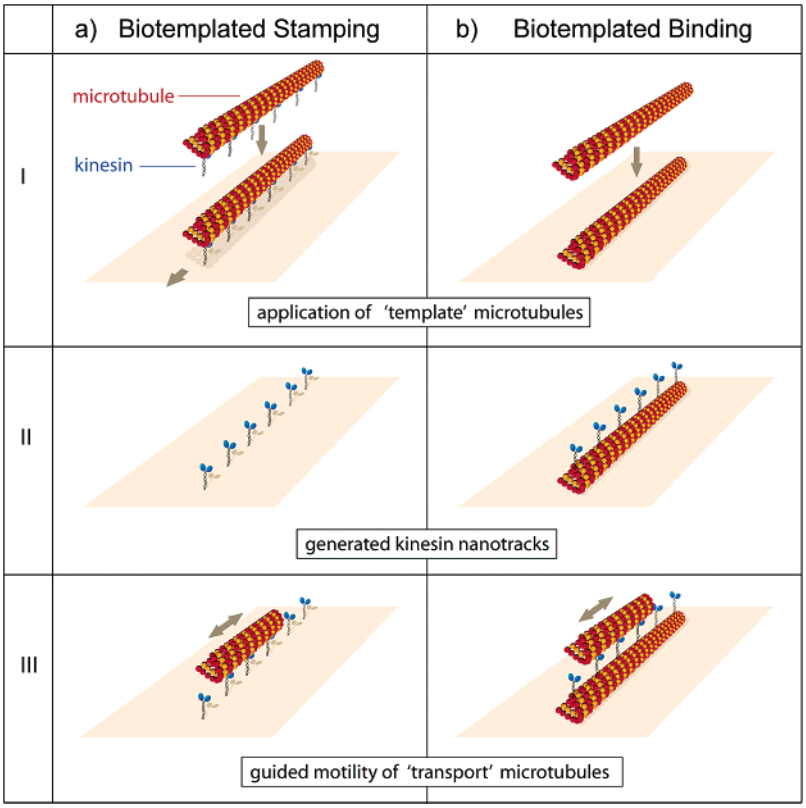

Figure 1. Methods of biotemplated nanopatterning. (a) Biotemplated stamping: kinesin molecules, which are bound in an oriented manner to the lattice of a template microtubule, are transferred onto the surface by a stamping process (I). After adsorption, the template microtubule is released when the deposited motor molecules propel the microtubule off the generated track in the presence of ATP (II). The same molecules will move and guide the transport microtubules (III). (b) Biotemplated binding: motor proteins are bound to a template microtubule that was previously immobilized on the surface (I and II). Transport microtubules then move specifically on the motor track, thereby sliding along the template microtubule (III).

optical microscope with a 100x oil immersion objective (NA = 1.3). For data acquisition, a back-illuminated CCD camera (MicroMax 512 BFT, Roper Scientific) was used in conjunction with a Metamorph imaging system (Universal Imaging Corp., Downington, PA). Images were acquired every second with an exposure time of 100 ms.

Figure 2 shows an example of the generation and the usage of a stamped kinesin "nanotrack".[11] Transport microtubules frequently bound to the stamped kinesin molecules and moved either precisely along or across the tracks. Sometimes, a microtubule walking across a track changed its direction and moved further along the track.

Analysis of the movement showed that microtubules preferably walked well-guided along the tracks (Figure 3a). Movement thereby occurred with equal likelihood in the direction in which the template microtubule had walked off the track or in the opposite direction. This behavior is expected because (i) the high torsional flexibility of the kinesin molecules[12] allows the kinesin heads to bind microtubules in any orientation, and (ii) the twofold symmetry of dimeric kinesin molecules[13] supports binding in either direction. Thus, only the orientation of a transport microtubule determines its direction of movement. Transport microtubules moved with similar speeds along the tracks in either direction. This speed was, moreover, independent of filament length and equaled the speed observed during walk-off (Table 1).

Once moving along a kinesin track, the guiding probability was larger than 80% ($n = 60$ microtubules), meaning that 80% of the transported microtubules followed the tracks to their ends. The reasons for not being guided were either the kinesin density on the track, which was in some cases insufficient for very short ($<1.5\ \mu$m) microtubules, or kinks in the tracks that microtubules could not follow. Taking into consideration the lengths of the smallest microtubules that reliably moved along the tracks, we estimate the motor density to be at least 0.7 functional kinesin molecules per micrometer.

To further characterize the motor tracks, we labeled the stamped kinesin molecules with kinesin antibodies that specifically targeted an epitope at the motor domain (C-terminus of the kinesin).[14] Fluorescein-5-isothiocyanate (FITC)-labeled secondary antibodies were then used to visualize the kinesin locations on the surface (Figure 3b). Although presumably not all kinesins were labeled by an antibody, the motors in the track appeared dense and homogeneously distributed. Because the kinesin antibodies bound specifically to the motor domains, the labeling provided further evidence for the orientation of the kinesin molecules: the heads or motor domains pointed away from

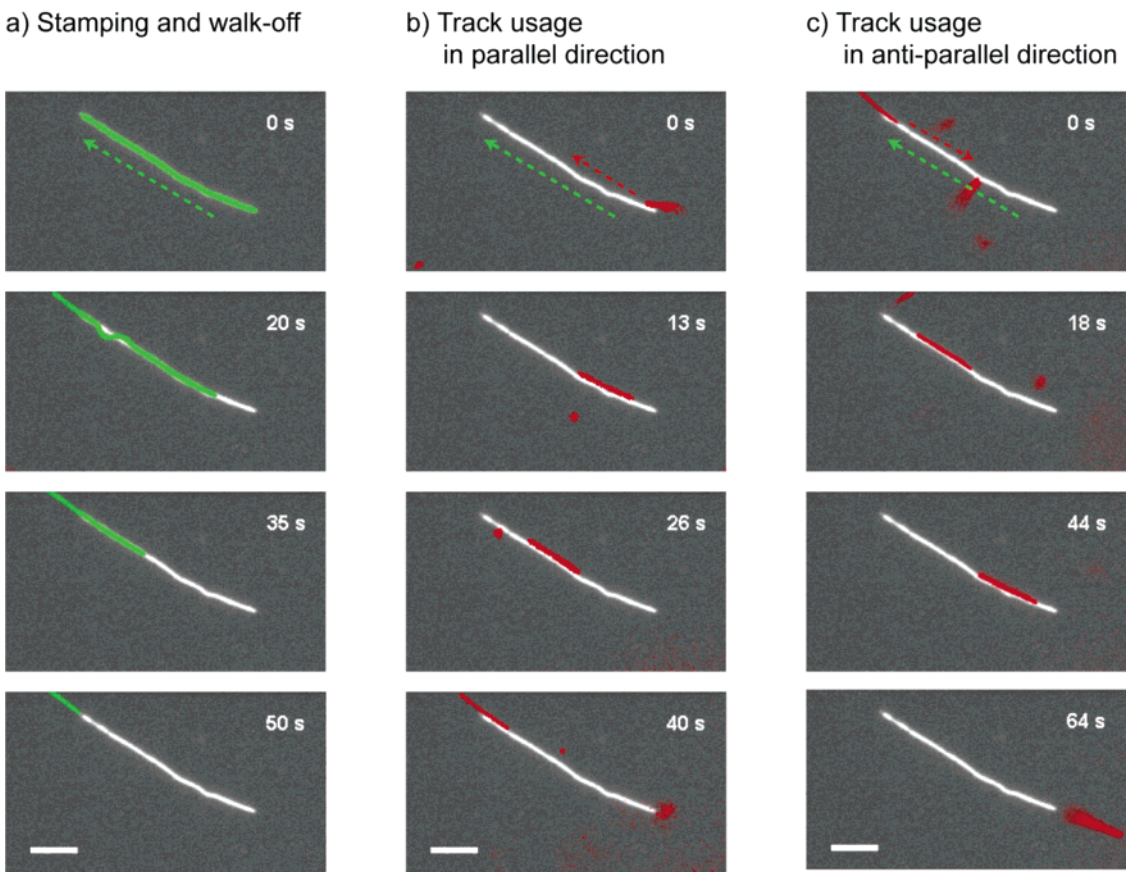

Figure 2. Generation and usage of stamped kinesin nanotracks. The location of the tracks is inferred from fluorescent micrographs of the kinesin-decorated template microtubules before ATP addition (shown in white). Real-time images of moving template and transport microtubules are superimposed in color. (a) Track generation. Immediately after ATP addition, the template microtubule (green) started to move one filament length, detached from the surface, and left a track of kinesin molecules on the surface. (b) A transport microtubule (red) followed the created track in the direction the template microtubule had walked off. (c) Another transport microtubule (red) followed the same track opposite to the walk-off direction and detached from the track after reaching its end. Scale bars represent 5 μm. Arrows indicate the directions of movement. See also Supporting Information movies S1 and S2.

the surface and were not attached to the substrate. This is of great importance for their biological activity and cannot be controlled by other direct protein patterning techniques, such as microcontact printing[15−20] or dip-pen nanolithography.[21]

Because kinesin molecules decorate the whole surface of the template microtubules (not shown in Figure 1a), we asked whether the nanotracks will be significantly broadened by the random substrate binding of those kinesin molecules released during walk-off. Evaluating fluorescence data, as presented in Figure 3b, we found that only few motors bound to the surface unassociated with the tracks and their density was too low to support motility. The labeling technique using the fluorescent antibodies also allowed us to quantitatively estimate the lateral width of the stamped tracks. Fitting the fluorescence intensity profile perpendicular to the track in Figure 3b by a Gaussian function (averaged over a microtubule length of 4 μm) yielded an apparent width (full width at half-maximum) of $w_{AB} = 451 \pm 6$ nm. Because of the limited optical resolution, this value represents the convolution of the real track width, w_{track}, with the one-dimensional point-spread function (width w_{PSF}) of our imaging system. If a Gaussian-like distribution for the locations of the track-forming kinesin molecules is assumed, then the track width can be estimated by $w_{track} = \sqrt{w_{AB}^2 - w_{PSF}^2}$ (deconvolution of two Gaussian functions[22]). Because the lateral width of a microtubule is at least 10 times smaller than the optical resolution of the imaging system, it is reasonable to approximate w_{PSF} by measuring the fluorescence intensity profile perpendicular to a fluorescein-labeled reference microtubule. Such a measurement yielded 386 ± 8 nm and the actual lateral width of the kinesin track was thus determined to be $w_{track} = 233 \pm 18$ nm. Although being a rough estimate, this value documents the narrow width of the track. However, it exceeds the width of the template microtubule by multiple times. Physical reasons for this broadness were presumably: (i) a nonperfect straightness of the template microtubule along the length over which the intensity profile was averaged, (ii) kinesin molecules (contour length of about 70 nm) that were bound on the sides of the template microtubule, and (iii) some broadening of the apparent track width due to the antibody labeling procedure. Moreover, because the localization accuracy of fluorescent objects is limited by the number of detected photons[23] the determined track width has to be considered as an upper limit.

Toward the usability of the stamped kinesin tracks for nanotechnological applications, we performed an additional experiment where nanocargo (streptavidin-coated quantum

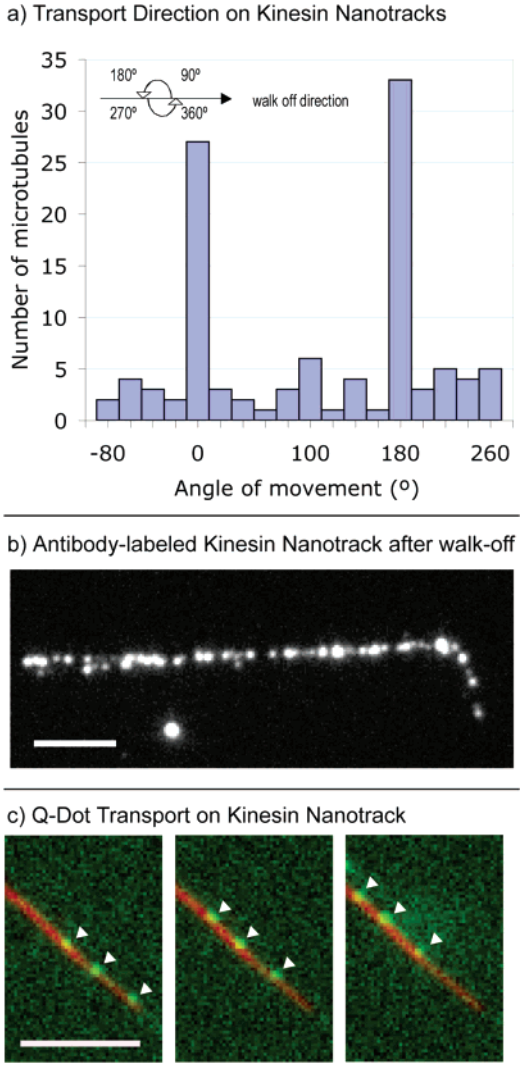

Figure 3. Evaluation and application of stamped kinesin nanotracks. (a) Distribution of movement directions on the created kinesin tracks with respect to the walk-off direction of the template microtubule. Although movement along the tracks (0 and 180°) is predominant, movement across the tracks is occurring at statistically distributed angles. (b) Fluorescent image of a kinesin track labeled with anti-kinesin and FITC-labeled secondary antibodies after the template microtubule had walked off. (c) Cargo transport along a kinesin nanotrack. Time-lapse images of three quantum dots (shown in green) that are bound to a motile transport microtubule (not shown) are superimposed to a fluorescent micrograph of the template microtubule before walk-off (shown in red, see also Supporting Information movie S3). Scale bars represent 5 μm.

dots bound to biotinylated microtubules) was transported along the tracks[24] (Figure 3c). Moreover, we observed that sometimes the tracks were used by multiple microtubules (with and without cargo) at the same time, occasionally even with microtubules passing each other in opposite direction (data not shown).

Our experiments on motor stamping confirm earlier studies in which motor proteins were deposited using filaments themselves to infer biophysical data on the flexibility of myosin heads[25] and on the behavior of oriented dynein arrays.[26] Here, we advanced this approach to kinesin motors and demonstrated the suitability of such motor tracks for the setup of guided nanotransport systems.

Table 1. Mean Gliding Velocity of Microtubules (Mean ± Standard Deviation, n = Number of Evaluated Microtubules) along Stamped Kinesin Nanotracks

walk-off (μm/s)	track usage (both directions) (μm/s)	track usage parallel to walk-off (μm/s)	track usage antiparallel to walk-off (μm/s)
0.62 ± 0.11 ($n = 39$)	0.59 ± 0.16 ($n = 39$)	0.56 ± 0.14 ($n = 22$)	0.63 ± 0.17 ($n = 17$)

Biotemplated binding of motor proteins was demonstrated using kinesin-1 and Ncd motors. In a first approach, biotinylated kinesin-1 molecules were bound via streptavidin to biotinylated template microtubules that were immobilized on the surface using specific antibodies.[27] Figure 4 shows examples of track usage by transport microtubules. To reduce the unspecific surface-binding of streptavidin and kinesin, it was crucial for us to block the glass surface with a polyethyleneglycol-terminated copolymer (Pluronic F127) after application of the antibodies. In experiments where the template microtubules were immobilized by tubulin antibodies (Figure 4a and b), free tubulin was added to the motility solution in order to saturate the microtubule binding sites of those antibodies and thus to avoid static binding of transport microtubules to the surface. A further and almost complete reduction of the undesirable interactions of the transport microtubules with the surface became possible when the template microtubules were immobilized by rhodamine antibodies and transport microtubules labeled with Alexa 488 were used. Using either immobilization procedure, the transport microtubules followed the tracks precisely in either direction. In total, we imaged 27 transport microtubules moving along biotinylated kinesin tracks. In all guiding events, the microtubules were neither observed to be pushed off the tracks by the motors nor did any microtubule move unspecifically on the surface.

In a second approach, Ncd motor molecules were bound to antibody-immobilized template microtubules[28] via their second, ATP-independent microtubule binding site.[29] Because template microtubules were frequently ruptured off the surface by Ncd motors that nonspecifically bound to the antibodies (control data with GFP-labeled Ncd not shown), we also fixed the template microtubules using glutaraldehyde. We found that this treatment, which preserves the microtubule structure,[30,31] also reduced nonspecific Ncd surface binding. Figure 5 shows examples of track usage by transport microtubules. Less than 10% of these microtubules ($n = 80$) moved across the tracks at arbitrary angles, some even becoming aligned with the tracks later on. Presumably, this alignment behavior, which is superior to the guiding achieved with kinesin-1 motors, originates from the fact that Ncd is a non-processive motor. Each Ncd molecule undergoes only one catalytic cycle per encounter with a microtubule, and about 4 Ncd molecules are required to work in concert to continuously move a microtubule.[32] Therefore, non-aligned movement of a transport microtubule across a Ncd track is rather unlikely. Non-processive microtubule motors might thus provide an advantage over processive ones in terms of

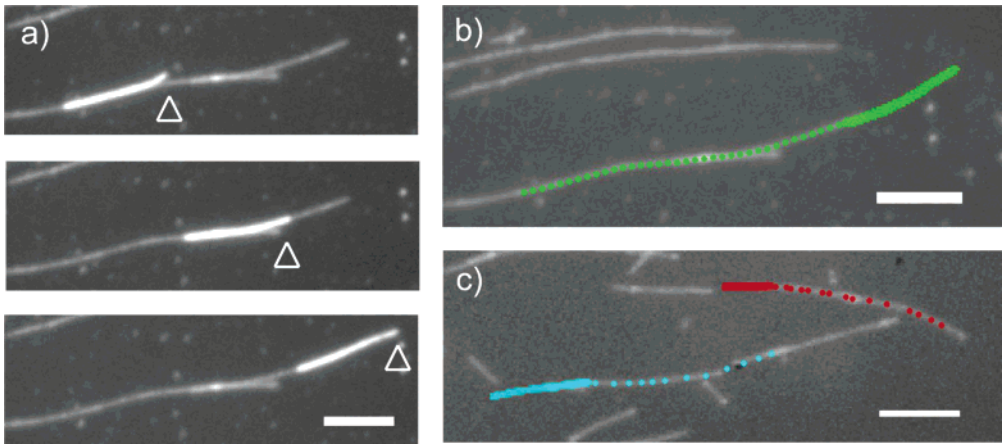

Figure 4. Usage of biotinylated kinesin tracks on surface-immobilized template microtubules. (a) Sequence of fluorescent images showing one transport microtubule (brightly labeled) moving on a template microtubule (dimly labeled) immobilized by tubulin antibodies. (b and c) Overlays of template microtubules (white) immobilized by tubulin antibodies (b) and rhodamine antibodies (c) with the paths of transport microtubules (colored). The paths were determined by automatic tracking of the ends of the motile transport microtubules. Scale bars represent 5 μm. See also Supporting Information movies S4 and S5.

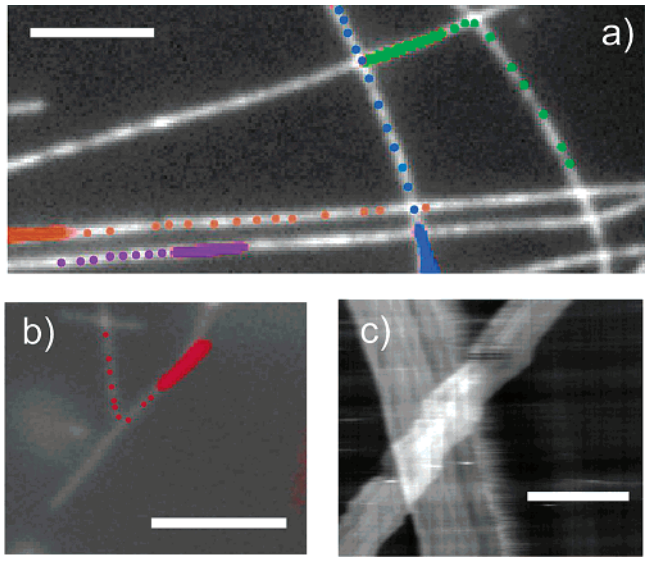

Figure 5. Usage of Ncd tracks on surface-immobilized template microtubules. (a) Overlay of template microtubules (white) immobilized and fixed by glutaraldehyde with the paths of transport microtubules (colored). (b) A microtubule takes a turn at a track crossing and gets redirected. (c) Kymograph (horizontal: fluorescence intensity profile along the template microtubule, vertical: time, 170 s) showing two transport microtubules that are sliding contemporaneously on one track in opposite directions. Scale bars represent 5 μm. See also Supporting Information movies S6−S8.

reliable guiding and transport on the nanoscale. The shortest moving microtubules that were propelled continuously along the Ncd tracks had lengths of 0.8 μm. On the basis of the fact that 4 motor molecules are necessary for continuous gliding[32] the motor density on the tracks was at least 5 functional Ncd molecules per micrometer.

We noted that moving microtubules were often tethered to the track with their trailing minus ends, whereas the leading plus ends frequently lifted up. This might be the result of a prolonged residence time of Ncd molecules at the microtubule minus ends, which we did in fact observe in experiments using GFP-labeled Ncd (data not shown). In terms of redirecting the movement of transport microtubules at track crossings and branching points, this behavior was found to be advantageous and reorientation onto the track geometry was even possible at T-like junctions (Figure 5b). Moreover, it was observed that microtubules walked in both directions along the tracks and were able to pass each other while sliding on the same track (Figure 5c). Because of the torsional flexibility in the Ncd molecules that are immobilized on the template microtubules, such bidirectional track usage was to be expected.

In summary, we demonstrated a novel approach for the nanometer structuring of surfaces with functional motor proteins. Biotemplated patterning allows the highly localized and oriented surface binding of proteins combined with low protein denaturation. This way, functional protein patterns of high surface density are producible. Other techniques to generate nanometer-wide structures of functional proteins on planar surfaces involve indirect-write patterning by dip-pen lithography.[33] Because dip-pen lithography offers the possibility to freely design the pattern layout, it would be interesting to generate motor tracks similar to the ones shown here by this method.

The created motor tracks showed that nanoscale-patterning is possible and can lead to reliable guiding of microtubules without topographical barriers. Recently, non-topographical patterning of surfaces with kinesin motors was demonstrated only in the micrometer range.[10,34] In those experiments, gliding microtubules could not be prevented from walking off the patterned tracks when they approached the boundaries at obtuse angles.[10] Because of the high flexural rigidity of the microtubules, in those cases the thermal energy of the system was not sufficient to bend the leading tips of the microtubules back onto the patterned motors. This problem is circumvented by the small width of our motor nanotracks, where the encounters of the microtubules with the boundaries are restricted to extremely shallow angles. Topography-free guiding, as demonstrated here, is expected to significantly ease the design and fabrication of microtubule-transport

systems and opens up the possibility to transport cargo of unlimited size, that is, without any constraints by the dimensions of topographic guiding channels. Moreover, biotemplated nanopatterning is a promising tool for in vitro studies on the individual and cooperative action of motor proteins as well as for the reconstitution of complex subcellular machineries in synthetic environments.

Acknowledgment. We thank H. Hess, J. Howard, C. Leduc, F. Nedelec, and V. Vogel for fruitful discussions. F. Ruhnow is acknowledged for the automated tracking of the microtubules, and C. Bräuer, for laboratory assistance. The biotinylated kinesin was expressed and purified by D. Drechsel and R. Lemaitre using a plasmid kindly provided by T. Surrey and J. Gelles. K. Skowronek is acknowledged for the His6-Ncd and His6-EGFP-Ncd constructs. The work was financially supported by the Max-Planck-Society, BMBF (grant 03N8712), UNESCO, BRAINS (L.H), and KBN 2P04C 13129 (A.A.K).

Supporting Information Available: Time-lapse movies of the generation and the usage of kinesin and Ncd nanotracks. This material is available free of charge via the Internet at http://pubs.acs.org.

References

(1) Hess, H.; Bachand, G. D.; Vogel, V. *Chemistry* **2004**, *10*, 2110−2116.
(2) Hess, H.; Clemmens, J.; Qin, D.; Howard, J.; Vogel, V. *Nano Lett.* **2001**, *1*, 235−239.
(3) Bachand, G. D.; Rivera, S. B.; Boal, A. K.; Gaudioso, J.; Liu, J.; Bunker, B. C. *Nano Lett.* **2004**, *4*, 817−821.
(4) Diez, S.; Reuther, C.; Dinu, C.; Seidel, R.; Mertig, M.; Pompe, W.; Howard, J. *Nano Lett.* **2003**, *3*, 1251−1254.
(5) Riveline, D.; Ott, A.; Julicher, F.; Winkelmann, D. A.; Cardoso, O.; Lacapere, J. J.; Magnusdottir, S.; Viovy, J. L.; Gorre-Talini, L.; Prost, J. *Eur. Biophys. J. Biophys. Lett.* **1998**, *27*, 403−408.
(6) Hess, H.; Matzke, C. M.; Doot, R. K.; Clemmens, J.; Bachand, G. D.; Bunker, B. C.; Vogel, V. *Nano Lett.* **2003**, *3*, 1651−1655.
(7) Clemmens, J.; Hess, H.; Howard, J.; Vogel, V. *Langmuir* **2003**, *19*, 1738−1744.
(8) Hiratsuka, Y.; Tada, T.; Oiwa, K.; Kanayama, T.; Uyeda, T. Q. P. *Biophys. J.* **2001**, *81*, 1555−1561.
(9) Moorjani, S. G.; Jia, L.; Jackson, T. N.; Hancock, W. O. *Nano Lett.* **2003**, *3*, 633−637.
(10) Clemmens, J.; Hess, H.; Lipscomb, R.; Hanein, Y.; Bohringer, K. F.; Matzke, C. M.; Bachand, G. D.; Bunker, B. C.; Vogel, V. *Langmuir* **2003**, *19*, 10967−10974.
(11) (a) Wild type kinesin-1 (full length *drosophila* expressed in bacteria and purified as described by Coy, D. L.; Wagenbach, M.; Howard, J. *J. Biol. Chem.* **1999**, *274*, 3667−3671) was mixed with rhodamine-labeled microtubules (labeling ratio: 1 rhodamine/3 unlabeled tubulin units) at a kinesin dimer to tubulin molar ratio of 1:8 in BRB80 buffer containing 10 μM taxol and 1 mM AMPPNP (BRB80TM) to form decorated microtubules. To achieve rapid binding and thus avoid cross-linking of microtubules, we performed the mixing while vortexing the solution. To remove any free, unbound kinesin molecules, 400 μL of the resulting solution (32 nM microtubules, 4 nM kinesin dimers) were centrifuged at 130 000g in a Beckmann airfuge for 2.5 min. The pellet was resuspended in 150 μL of BRB80TM. (b) A casein-containing solution (0.5 mg/mL in BRB80) was perfused into the flow cell and allowed to adsorb to the surface for 5 min to reduce the denaturation of kinesin and to prevent the sticking of microtubules. Then the solution containing the decorated microtubules was perfused. After 5−10 min, the flow cell was washed with BRB80TM containing anti-bleaching reagents (20 mM D-Glucose, 0.020 mg/mL glucose oxidase, 0.008 mg/mL catalase and 1% 2-mercaptoethanol). To walk the microtubules off the surface, we perfused an ATP anti-bleaching solution (containing 1 mM Mg-ATP instead of AMPPNP) into the cell. In the last step, motility solution containing microtubules (∼30 nM tubulin) and ATP anti-bleaching solution was added to the cell.
(12) Hunt, A. J.; Howard, J. *Proc. Natl. Acad. Sci. U.S.A.* **1993**, *90*, 11653−11657.
(13) Howard, J. *Annu. Rev. Physiol.* **1996**, *58*, 703−729.
(14) Antibody labeling of the kinesin tracks was performed by perfusing 1.25 μg/mL anti-kinesin (mouse monoclonal SUK4; Cytoskeleton) in PB100BA buffer (100 mM phosphate buffer; pH = 7.5, containing 1 mg/mL BSA and 1 mM ATP) into the flow cell instead of the motility solution. After one hour incubation, we rinsed the cell with PB100BA. FITC-labeled goat anti-mouse IgG (whole molecule; 17 μg/mL in PB100BA; Sigma-Aldrich) was added as secondary antibody. After another 45 minutes of incubation, the solution was exchanged with an ATP anti-bleaching solution.
(15) Odom, T. W.; Love, J. C.; Wolfe, D. B.; Paul, K. E.; Whitesides, G. M. *Langmuir* **2002**, *18*, 5314−5320.
(16) Renault, J. P.; Bernard, A.; Bietsch, A.; Michel, B.; Bosshard, H. R.; Delamarche, E.; Kreiter, M.; Hecht, B.; Wild, U. P. *J. Phys. Chem. B* **2003**, *107*, 703−711.
(17) Andrade, J. D.; Hlady, V. *Adv. Polym. Sci.* **1986**, *79*, 1−63.
(18) Graber, D. J.; Zieziulewicz, T. J.; Lawrence, D. A.; Shain, W.; Turner, J. N. *Langmuir* **2003**, *19*, 5431−5434.
(19) Biasco, A.; Pisignano, D.; Krebs, B.; Pompa, P. P.; Persano, L.; Cingolani, R.; Rinaldi, R. *Langmuir* **2005**, *21*, 5154−5158.
(20) Bergkvist, M.; Carlsson, J.; Karlsson, T.; Oscarsson, S. *J. Colloid Interface Sci.* **1998**, *206*, 475−481.
(21) Ginger, D. S.; Zhang, H.; Mirkin, C. A. *Angew. Chem. Int. Ed.* **2004**, *43*, 30−45.
(22) Bracewell, R. *The Fourier Transform and Its Applications*, 3rd ed; McGraw-Hill: New York, 1999, pp 25−50 and 243−244.
(23) Thompson, R. E.; Larson, D. R.; Webb, W. W. *Biophys. J.* **2002**, *82*, 2775−2783.
(24) For the cargo transport experiment, we perfused rhodamine-biotin-labeled transport microtubules (labeling ratio: 3 rhodamine/4 biotin/9 unlabeled tubulin units; ∼30 nM tubulin) in AMPPNP anti-bleaching solution into the cell instead of the motility solution. After they had bound to the generated kinesin tracks, streptavidin-coated quantum dots (525 nm emission, 20 000x diluted; Invitrogen) were loaded onto the transport microtubules. Finally, an ATP anti-bleaching solution was added to start the movement of the cargo-loaded transport microtubules.
(25) Toyoshima, Y. Y.; Toyoshima, C.; Spudich, J. A. *Nature* **1989**, *341*, 154−156.
(26) Mimori, Y.; Miki-Noumura, T. *Cell Motil. Cytoskeleton* **1994**, *27*, 180−191.
(27) Beta-tubulin (TUB 2.1, 4 μg/mL; Sigma) or tetramethylrhodamine (4 μg/mL; Molecular Probes) antibodies were adsorbed for 5 min onto a hydrophobic glass surface that was previously treated with dichlorodimethylsilane. The surface was then blocked against unspecific protein binding by Pluronic F127 (1% dissolved in BRB80). Rhodamine-biotin-labeled microtubules (labeling ratio: 3 rhodamine/4 biotin/9 unlabeled tubulin units) were polymerized, and unpolymerized tubulin was removed by 5 min centrifugation at 180 000g in a Beckmann airfuge. The pellet was resuspended in BRB80 containing 10 μM taxol to a final tubulin concentration of 80 nM.; this solution was added to the flow cell in order to bind these template microtubules to the antibodies on the substrate surface. In the next steps, first fluorescein labeled streptavidin (10 μg/mL in BRB80, Pierce) was perfused into the flow cell. Secondly, biotinylated kinesin K401-BIO (Berliner, E.; Young, E. C.; Anderson, K.; Mahtani, H. K.; Gelles, J. *Nature* **1995**, *373*, 718−721.) (2.5 μg/mL in BRB80, containing 10 μM taxol, 0.5 mg/mL casein and 20 mM ATP) was added. The flow cell was rinsed with ATP anti-bleaching solution, and microtubule containing motility solution was perfused. In experiments with tubulin antibodies, free tubulin was added to the motility solution with a final concentration of 20 μg/mL. In experiments where tetramethylrhodamine antibodies were used to immobilize template microtubules, the transport microtubules were labeled with Alexa-488.
(28) (a) Penta-his antibodies (10 μg/mL; Qiagen) were adsorbed onto the hydrophobic glass surface of the flow cell. After blocking the surface with Pluronic F127 (1% dissolved in BRB80), his-tagged kinesin was bound to these antibodies. Dimly rhodamine-labeled microtubules (labeling ratio: 1 rhodamine/5 unlabeled tubulin units) in BRB80TM were then immobilized on the kinesin-coated surface. To remove the unbound microtubules, we rinsed the flow cell with BRB80TM.

Bound microtubules were cross-linked for 15 min in a 0.1% solution of glutaraldehyde in BRB80TM. Subsequently, a 15 min treatment of the cell with 0.1 M glycine was performed to block free aldehyde groups. (b) For the preparation of Ncd, single colony BL21 (DE3) *E. Coli* strain transformed with plasmid HisEGFPNcd (a gift of K. Skowronek) encoding His6-EGFP-Ncd was grown over night at 37° C in luria bertani medium containing 50 μg/mL kanamycin and used to inoculate 2 L of new medium. Expression of Ncd was induced 14 h with 1 mM IPTG at 22° C. Cells were harvested by centrifugation at 3000g for 10 min, washed in buffer A (10 mM HEPES pH 7.2, 0.3 M NaCl, 1 mM $MgCl_2$, 10 mM 2-mercaptoethanol), and centrifuged again at 6000g for 20 min; the supernatant was discarded and the pellet was frozen. Bacteria were lysed by a French Press (Thermo-Spectronic) in buffer A + 10 mM imidazole with protease inhibitors (1 mM phenylmethanesulfonyl fluoride, 1 μg/mL leupeptin, 1 μg/mL pepstatin, and 2 μg/mL aprotinin (all from Sigma)). The lysate was centrifuged at 30 000g for 20 min, and the supernatant was loaded on a HIS-TRAP column (DNA Gdansk, Poland). The column was washed with buffer A + 50 mM imidazole and the protein was eluted with 10 mM HEPES pH 7.2, 500 mM imidazole, 0.1 M NaCl, 1 mM $MgCl_2$, 10 mM 2-mercaptoethanol. The peak fractions were frozen in the presence 10% sucrose and 10 μM ADP. (c) Ncd was diluted in BRB20 buffer (20 mM potassium PIPES, pH 6.9, 1 mM EGTA, 1 mM $MgCl_2$) containing 10 μM taxol, 1 mM ATP, and 100 mM NaCl. This solution was centrifuged for 5 min at 180 000g in a Beckmann airfuge to remove clustered molecules and then added to the fixed microtubules in the flow cell. Finally, after washing twice with BRB20 containing 10 μM taxol and 1 mM ATP, motility solution containing microtubules (~30 nM tubulin) and ATP anti-bleaching solution (in BRB20) was flown in.

(29) Karabay, A.; Walker, R. A. *Biochemistry* **1999**, *38*, 1838−1849.
(30) Turner, D.; Chang, C.; Fang, K.; Cuomo, P.; Murphy, D. *Anal. Biochem.* **1996**, *242*, 20−25.
(31) Bohm, K. J.; Stracke, R.; Muhlig, P.; Unger, E. *Nanotechnology* **2001**, *12*, 238−244.
(32) deCastro, M. J.; Ho, C. H.; Stewart, R. J. *Biochemistry* **1999**, *38*, 5076−5081.
(33) Lee, S. W.; Oh, B. K.; Sanedrin, R. G.; Salaita, K.; Fujigaya, T.; Mirkin, C. A. *Adv. Mater.* **2006**, *18*, 1133−1136.
(34) Hess, H.; Clemmens, J.; Matzke, C. M.; Bachand, G. D.; Bunker, B. C.; Vogel, V. *Appl. Phys. A (Materials Science Processing)* **2002**, *75*, 309−313.

NL060922L